

Interfacial Phase Transition of an Environmentally Responsive Elastin Biopolymer Adsorbed on Functionalized Gold Nanoparticles Studied by Colloidal Surface Plasmon Resonance

Nidhi Nath and Ashutosh Chilkoti*

Contribution from the Department of Biomedical Engineering, Duke University, Box 90281, Durham, North Carolina 27708

Received January 25, 2001

Abstract: The change in optical properties of colloidal gold upon aggregation has been used to develop an experimentally convenient colorimetric method to study the interfacial phase transition of an elastin-like polypeptide (ELP), a thermally responsive biopolymer. Gold nanoparticles, functionalized with a self-assembled monolayer (SAM) of mercaptoundecanoic acid onto which an ELP was adsorbed, exhibit a characteristic red color due to the surface plasmon resonance (SPR) of individual colloids. Raising the solution temperature from 10 °C to 40 °C thermally triggered the hydrophilic-to-hydrophobic phase transition of the adsorbed ELP resulting in formation of large aggregates due to interparticle hydrophobic interaction. Formation of large aggregates caused a change in color of the colloidal suspension from red to violet due to coupling of surface plasmons in aggregated colloids. The surface phase transition of the ELP was reversible, as seen from the reversible change in color upon cooling the suspension to 10 °C. The formation of colloidal aggregates due to the interfacial phase transition of adsorbed ELP was independently verified by dynamic light scattering of ELP-modified gold colloids as a function of temperature. Colloidal SPR provides a simple and convenient colorimetric method to study the influence of the solution environment, interfacial properties, and grafting method on the transition properties of ELPs and other environmentally responsive polymers at the solid–water interface.

Introduction

Extrinsic, triggered control of interfacial properties is attractive for the development of regenerable biosensors and proteomic chips, interfacial control of microfluidics^{1,2} in bio-MEMS devices, and the design of biomaterials^{3,4} that enable the dynamic (temporally modulated) presentation of cell-specific ligands on their surface. One approach to the fabrication of surfaces with controlled modulation of interfacial properties (e.g. wettability) involves the adsorption or grafting of “smart” (environmentally responsive) polymers onto surfaces.

A number of studies have reported a thermally reversible change in the hydrophobicity of surfaces grafted with poly(*N*-isopropyl acrylamide) (PNIPAAm), a prototypical “smart” polymer that exhibits a lower critical solution temperature (LCST) transition in aqueous solution.^{5–7} Potential interfacial applications of this effect have also been recently demonstrated in thermally switchable cell culture of anchorage-dependent

mammalian cells,^{8,9} and as a method to control bacterial biofouling by thermally triggered desorption of attached bacteria from surfaces.¹⁰ Our laboratory is similarly interested in the design of interfacial applications of a genetically encoded “smart” biopolymer, an elastin like polypeptide (ELP), that potentially offers several advantages compared to PNIPAAm.

ELPs are a class of synthetic polypeptides consisting of a Val-Pro-Gly-Xaa-Gly repeat unit, where the “guest” residue Xaa can be any of the natural amino acids except Proline.¹¹ ELPs exhibit a reversible hydrophilic–hydrophobic phase transition in aqueous solution, in response to small changes in the solution environment (e.g. temperature, pH, or ionic strength).¹² The inverse phase transition of ELPs is analogous to the LCST transition exhibited by PNIPAAm and its copolymers in aqueous solution. ELPs are especially attractive for many interfacial applications, because they are genetically encodable, which enables important macromolecular properties such as sequence, chain length, and stereochemistry to be controlled to an extent that is impossible with synthetic polymers. Furthermore, the type, number, and location of reactive sites on the polypeptide chain can also be precisely specified, which allows control of the grafting of these polypeptides to the surface.

* Address correspondence to this author. E-mail: chilkoti@duke.edu. Phone: (919) 660-5373. Fax: (919) 684-4488.

(1) Beebe, D. J.; Moore, J. S.; Yu, Q.; Liu, R. H.; Kraft, M. L.; Jo, B.; Devadoss, C. *Proc. Natl. Acad. Sci.* **2000**, *97*, 13488–13493.

(2) Zhao, B.; Moore, J. S.; Beebe, D. J. *Science* **2001**, *291*, 1023–1026.

(3) Sakiyama-Elbert, S. E.; Hubbell, J. A. *J. Controlled Release* **2000**, *65*, 389–402.

(4) Yousaf, M. N.; Houseman, B. T.; Mrksich, M. *Angew. Chem., Int. Ed.* **2001**, *40*, 1093–1096.

(5) Takei, Y. G.; Aoki, T.; Sanui, K.; Ogata, N.; Sakurai, Y.; Okano, T. *Macromolecules* **1994**, *27*, 6163–6166.

(6) Yakushiji, T.; Sakai, K. *Langmuir* **1998**, *14*, 4657–4662.

(7) Liang, L.; Feng, X.; Liu, J.; Rieke, P. C.; Fryxell, G. E. *Macromolecules* **1998**, *31*, 7845–7850.

(8) Kushida, A.; Yamato, M.; Konno, C.; Kikuchi A.; Sakurai, Y.; Okano, T. *J. Biomed. Mater. Res.* **2000**, *51*, 216–223.

(9) Uchida, K.; Kwon, O. H.; Ito, E.; Aoyagi, T.; Kikuchi, A.; Yamato, M.; Okano, T. *Macromol. Rapid Comm.* **2000**, *21*, 169–173.

(10) Ista, L. K.; Perez-Luna, V. H.; Lopez, G. P. *Appl. Environ. Microbiol.* **1999**, *65* (4), 1603–1609.

(11) Urry, D. W. *Prog. Biophys. Mol. Bio.* **1992**, *57*, 23–57.

(12) Urry, D. W. *J. Phys. Chem. B* **1997**, *101*, 11007–11028.

Future technological applications of ELPs and other environmentally responsive polymers will require detailed elucidation of the factors that likely control the interfacial phase transition, such as chain length of the polymer and its surface density, the method of coupling, and the interfacial energy and chemistry of the substrate. A critical limitation in the effective realization of these potential applications is an easy to use and reliable technique to study the phase transition of these polymers on surfaces and its dependence on surface properties and the immobilization method. The most commonly used technique, the measurement of dynamic contact angles by Wilhelmy plate experiment,^{5,13} is experimentally difficult to perform as a function of solution conditions (e.g., temperature, ionic strength, or pH), and the results are often ambiguous. Furthermore, it involves repeated exposure of the surface to air, which, we have observed, can irreversibly alter the interaction between the surface and the biopolymer, and hence its transition.¹⁴

We have discovered that the physicochemical properties of adsorbed and covalently grafted "smart" polymers can be conveniently studied in situ in an aqueous environment of interest by colloidal surface plasmon resonance (colloidal SPR) of gold nanoparticles¹⁵ as a function of solution conditions. This method exploits the dramatic change in the color, due to surface plasmon absorbance, of colloidal gold onto which the polymer is adsorbed or covalently grafted, as a function of environmental, solution conditions. We report in this paper the use of this method to study the phase transition of an ELP adsorbed at the solid-water interface.

Experimental Section

ELP Design and Synthesis. An ELP with a MW of 71 kDa was synthesized by overexpression of a plasmid-borne synthetic gene of the ELP in *Escherichia coli*, as reported earlier.^{16,17} Briefly, the ELP was designed to have a target transition temperature (T_i) of around 40 °C in solution by incorporation of Val, Gly, and Ala in a 5:3:2 ratio, respectively, at the fourth, guest residue position of the pentapeptide.¹⁸ Next, a synthetic gene encoding 10 pentapeptides of the ELP was self-assembled by annealing chemically synthesized oligonucleotides (Integrated DNA Technologies, Coralville, IA). The monomer gene was then oligomerized by a stepwise, head-to-tail DNA oligomerization procedure¹⁹ to provide a gene encoding 180 ELP pentapeptides in pUC19 (New England Biolabs, Beverly, MA). The oligomerized gene was then excised from pUC19 and ligated into a modified pET25b expression vector (Novagen Inc., Madison, WI). The expression vector contained translation, initiation, and termination codons, and codons for short leading (Ser-Lys-Gly-Pro-Gly) and trailing (Trp-Pro) sequences. Standard molecular biology protocols were used for all DNA manipulations.²⁰

The ELP was expressed in the *E. coli* strain BLR (DE3) (Novagen). The ELP was purified from other *E. coli* proteins in the soluble fraction of the cell lysate by inverse transition cycling.¹⁶ The ELP was characterized for purity and MW by SDS-PAGE and visualized by copper staining.²¹

(13) *Polymer Surface Dynamics*; Andrade, J. D., Ed.; Plenum Press: New York, 1988.

(14) Nath, N.; Chilkoti, A. Unpublished results.

(15) Link, S.; El-Sayed, M. A. *Int. Rev. Phys. Chem.* **2000**, *19*, 409–453.

(16) Meyer, D. E.; Chilkoti, A. *Nature Biotechnol.* **1999**, *17*, 1112–1115.

(17) Meyer, D. E.; Kong, G. A.; Dewhirst, M. W.; Zalutsky, M. R.; Chilkoti, A. *Cancer Res.* **2001**, *61*, 1548–1554.

(18) Urry, D. W.; Luan, C. H.; Parker, T. M.; Gowda, D. C.; Prasad, K. U.; Reid, M. C.; Safavy, A. *J. Am. Chem. Soc.* **1991**, *113*, 4346–4348.

(19) Meyer, D. E.; Chilkoti, A. Manuscript in preparation.

(20) Ausubel, F. M.; Brent, R.; Kingston, R. E.; Moore, D. H.; Siedman, J. G.; Smith, J. A.; Struhl, K. *Current Protocols in Molecular Biology*; John Wiley & Sons: New York, 1995.

(21) Lee, C.; Levin, A.; Branton, D. *Anal. Biochem.* **1987**, *166*, 308–312.

Characterization of the Inverse Phase Transition of ELP in Solution. The inverse phase transition of the ELP was characterized in solution by monitoring the optical density at 350 nm as a function of temperature on a UV-visible spectrophotometer equipped with a multicell thermoelectric temperature controller (Cary 300Bio; Varian Instruments). Reversibility of the transition was examined by first heating an ELP solution in 10 mM sodium phosphate buffer, pH 7.2 (PB), typically from 10 to 50 °C at a rate of 1 °C/min, and then cooling the solution to 10 °C at the same rate.

Synthesis and Characterization of ELP-Functionalized Colloidal Gold. Gold colloids were prepared by sodium citrate reduction of $\text{HAuCl}_4 \cdot 3\text{H}_2\text{O}$ (Aldrich).²² All glassware used for synthesis of colloids was cleaned using aqua regia (3:1 HCl:HNO₃), rinsed extensively with water, and dried in an oven at 100 °C. A 180 mL sample of distilled water was brought to a vigorous boil with rapid stirring in a 500 mL round-bottom flask fitted with a reflux condenser and 10 mL of aqueous 1 mg/mL HAuCl_4 was added quickly. Once the solution resumed boiling, 10 mL of a 10 mg/mL $\text{C}_6\text{H}_5\text{O}_7\text{Na}_3 \cdot 2\text{H}_2\text{O}$ (trisodium citrate, Sigma) solution in water was added quickly with continued stirring, which resulted in the solution turning red within 20 min. The colloidal gold suspension was cooled to room temperature and filtered through a 0.2 μm filter (Corning, NY). The diameter of the colloids was determined by transmission electron microscopy (TEM). A small drop of the colloidal gold suspension was placed on a lysine-coated Formvar grid, and excess solution was removed by wicking using a filter paper. The grid was then dried in air and imaged on a Philips 400S transmission electron microscope. The accelerating voltage was 80 kV. The size of the gold colloids was determined by analysis of TEM images of gold colloids ($n = 120$).

For formation of a mercaptoundecanoic acid (MUA) SAM, the colloidal suspension was dialyzed against 1 mM NaOH and incubated overnight with an equal volume of a 0.2 mM solution of MUA (Aldrich) in absolute ethanol. For ELP adsorption, 3 mL of a MUA-modified colloid was washed twice with a 1:1 mixture of 1 mM NaOH and ethanol and twice with 1 mM NaOH to remove ethanol and residual thiol. After a final wash, colloids were incubated with a 1 mg/mL solution of ELP in PB for 2 h, washed thrice with PB, and finally suspended in PB. For each wash step, the colloids were incubated with the wash solution at room temperature and recovered from solution by centrifugation at 14 000 g for 5 min.

Characterization of Colloidal Aggregation by UV-Visible Spectrophotometry. The temperature-dependent aggregation of ELP-modified colloidal gold was monitored by measuring the absorbance spectrum as a function of temperature using a temperature-controlled spectrophotometer (Cary 300Bio), equipped with a thermoelectrically controlled multicell holder and temperature probe. The temperature was varied in 5 °C increments over 10–40 °C. A thermocouple was used to monitor the temperature of the solution in the cuvette. The absorbance spectra were collected between 350 and 750 nm and the normalized integrated area (NIA) between 600 and 750 nm was used as an indicator of aggregate formation. The NIA is defined as follows: $\text{NIA}(T) = (B_T - A)/A$, where A is the initial integrated absorbance between 600 and 750 nm at 10 °C before commencement of thermal cycling, and B_T is the integrated absorbance between 600 and 750 nm at temperature T .

Dynamic Light Scattering. Dynamic light scattering (DLS) was performed on a temperature-controlled DynaPro-LSR dynamic light scattering instrument (Protein Solutions, Charlottesville, VA) equipped with an 830 nm wavelength semiconductor laser. Scattered light was collected at 90°. Fifty data points, each with a 5 s collection time, were acquired at 5 °C intervals as a solution of ELP-modified colloidal gold in PB was heated from 15 to 40 deg C. Samples were left to equilibrate for 5 min after the block temperature reached the set temperature. The data were analyzed by a regularization algorithm for spherical particles (Protein Solutions' Dynamics software, version 5.26.37).

Surface Plasmon Resonance Measurement. Conventional SPR studies on planar gold samples were performed on a BicaoreX instrument (Biacore AB, Sweden). The substrates for planar SPR studies were prepared by thermal evaporation of a 2 nm layer of Cr on glass

(22) Weisbecker, C. S.; Meritt, M. V.; Whitesides, G. M. *Langmuir* **1996**, *12*, 3763–3772.

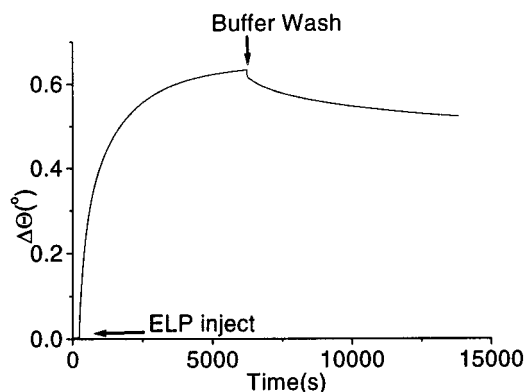


Figure 1. Adsorption of ELP on a COOH-terminated SAM of MUA on a planar gold substrate, studied by conventional SPR.

coverslips followed by 50 nm gold. Gold-coated glass coverslips were cut into 1×1 cm pieces and incubated overnight in a 1 mM solution of MUA in ethanol. Functionalized gold chips were glued to empty Biacore cassettes using water-insoluble double-sided sticky tape (3M Inc.) and docked into the instrument. The adsorption of ELP on MUA SAM was performed by injecting a 1 mg/mL solution of ELP in PB at a flow rate of $1.0 \mu\text{L}/\text{min}$ for 100 min at 25°C , followed by injecting PB to monitor the desorption of ELP at the same experimental conditions for 120 min.

Results and Discussion

Characterization of ELP Adsorption on MUA SAM. We studied the adsorption kinetics of the ELP on a MUA SAM on a flat gold substrate by conventional SPR (Figure 1). The adsorption of ELP exhibited heterogeneous kinetics: initial rapid adsorption of ELP was followed by much slower adsorption kinetics as the surface was saturated with ELP. The injection of buffer resulted in an initial sharp drop in the SPR response due to displacement of the protein solution by buffer with a lower refractive index, followed by a gradual decrease in the signal due to desorption of loosely bound protein. After the initial sharp drop due to changes in the bulk refractive index, the signal decreased by $\sim 10\%$ of its maximum value over the first hour, and only by 3% over the next hour, indicating that the ELP is strongly bound to the MUA SAM over the time scale of the colloidal SPR measurements. We calculated the amount of protein adsorbed on the SAM to be $\sim 5.0 \text{ ng}/\text{mm}^2$ by assuming that a change in 0.1° in the SPR response corresponds to $\sim 1.0 \text{ ng}/\text{mm}^2$ of adsorbed ELP.²³

The stable adsorption of a significant amount of ELP is somewhat surprising, in light of the fact that the MUA SAM provides a hydrophilic surface with a water contact angle of less than 10° . Under our experimental conditions, the MUA surface is negatively charged and the ELP has a net positive charge ($pI = 9.0$). The ELP has three charged groups distributed in a highly directional manner along the polymer chain: there are two positive charges located at the N-terminal segment of the polypeptide, one from the N-terminal amine and another from a Lysine, located at the third position in the amino acid sequence, while the negatively charged carboxyl group is located at C-terminus of the ELP. Hence, we suggest that the electrostatic interactions play an important role in ELP adsorption to the MUA surface.

Characterization of Phase Transition of ELP Adsorbed on a MUA SAM on Gold Colloids. The size of gold colloids used for our experiments, as determined by TEM of gold

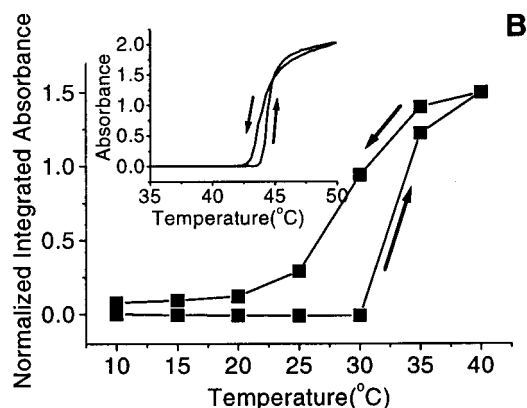
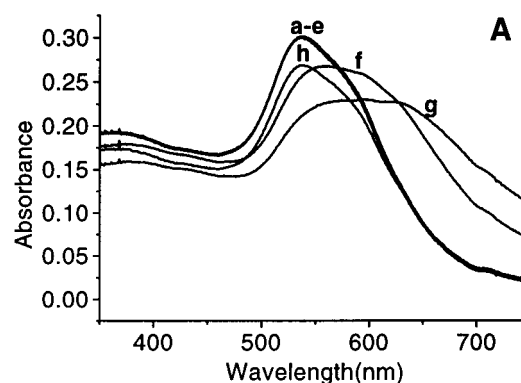


Figure 2. (A) Absorbance spectrum of adsorbed ELP on colloidal gold functionalized with a MUA SAM (Au-ELP) at various temperatures. (a–e) overlaid spectra at 10, 15, 20, 25, and 30, (f) 35, (g) 40 $^\circ\text{C}$ and (h) after cooling the colloid from 40 $^\circ\text{C}$ to 10 $^\circ\text{C}$. (B) Normalized integrated absorbance from 600 to 750 nm (NIA) of Au-ELP as a function of temperature. The NIA shows a sharp increase at 30 $^\circ\text{C}$ indicating the occurrence of the phase transition of adsorbed ELP. The aggregation of an aqueous solution of ELP as a function of temperature is shown in the inset for comparison

nanoparticles, was $32.3 \pm 7.5 \text{ nm}$ ($n = 120$). Assuming complete conversion of the HAuCl_4 to gold, we calculated a colloid concentration of 140 pM in solution. The UV–visible spectrum of unmodified colloidal gold exhibited a surface plasmon absorbance peak at 528 nm. Adsorption of the ELP on the colloids resulted in a shift in the peak absorbance to 535 nm, as shown in Figure 2A, that we believe is due to the change in the refractive index of medium surrounding the colloids due to the presence of adsorbed protein and buffer.²⁴

The phase transition behavior of adsorbed ELP on MUA-modified gold colloids (Au-ELP) was monitored by measuring the absorbance spectrum as the solution temperature was cycled between 10 and 40 $^\circ\text{C}$. The spectrum of Au-ELP displayed an absorbance maximum at 535 nm at 10 $^\circ\text{C}$, and the spectrum did not change as the solution temperature was increased in 5 deg C increments from 10 to 30 $^\circ\text{C}$. With further increase in temperature beyond 30 $^\circ\text{C}$, the absorbance decreased at lower wavelengths, while simultaneously increasing at longer wavelengths, along with a red shift of the peak wavelength and broadening of the spectrum. We also measured the temperature-dependent absorbance of the following control samples: bare colloidal gold, a MUA SAM on colloidal gold, and adsorbed BSA on an MUA SAM on colloidal gold. We chose BSA as a negative control, because no significant conformational change

(23) Lahiri, J.; Isaacs, L.; Tien, J.; Whitesides, G. M. *Anal. Chem.* **1999**, *71*, 777–790.

(24) Storhoff, J. J.; Lazarides, A. A.; Mucic, R. C.; Chad, A.; Mirkin, C. A.; Letsinger, R. L.; Schatz, G. C. *J. Am. Chem. Soc.* **2000**, *122*, 4640–4650.

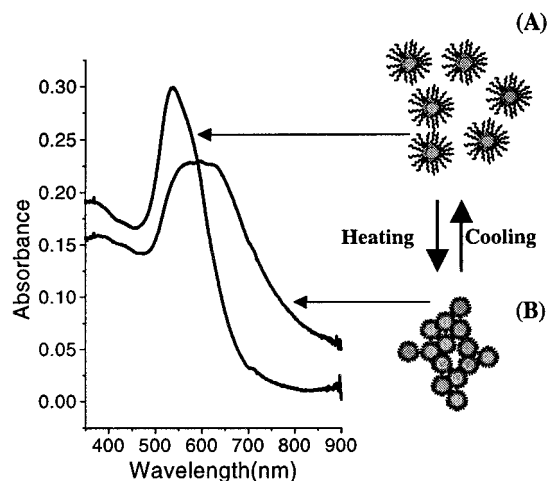


Figure 3. Schematic of reversible aggregation of gold nanoparticles caused by environmentally triggered phase transition of adsorbed ELP: (A) Au-ELP in the hydrophilic phase with spectra typical of isolated gold colloid and (B) aggregates which exhibit a red shift in their absorbance spectra compared to that of individual colloid in part A.

has been reported for adsorbed BSA in the range of 10–40 °C.^{25,26} There was no change in the absorbance spectrum of each control as a function of temperature, which strongly suggested that the optical changes observed for Au-ELP are due to the temperature-dependent phase transition of the adsorbed ELP.

We attribute these dramatic spectral changes as a function of temperature to the long-range coupling of surface plasmons. Below the phase transition temperature, the Au-ELP colloids in suspension have an average interparticle distance several times greater than the colloid radius, and hence appear red due to surface plasmon resonance of individual colloidal particles. Upon raising the temperature of an Au-ELP suspension, the adsorbed ELP undergoes an intramolecular hydrophilic–hydrophobic transition, resulting in increased hydrophobic interaction of the colloids and subsequently formation of large aggregates (Figure 3). The interparticle distance of the colloids in the aggregated state approaches the colloidal radius, and long-range coupling of plasmons from individual colloidal particles is observed, which results in a red-shift in the absorbance spectrum, and the suspension consequently appears violet. Cooling the suspension back to 10 °C causes the ELP to transition back to the hydrophilic state, which dissociates the colloidal aggregates, and returns the absorbance maximum to 535 nm (Figure 2A, curve h). Similar spectral changes have been experimentally observed,²⁷ and theoretically explained²⁸ for the formation of colloidal aggregates due to hybridization of oligonucleotide-linked gold colloids with a complementary oligonucleotide sequence.

We have also investigated the surface phase transition for covalently grafted ELPs on COOH-terminated SAMs. The phase transition behavior of adsorbed and covalently grafted ELPs is similar, but differ in the degree of reversibility, with adsorbed ELPs displaying significantly greater reversibility than covalently immobilized ELP. A detailed comparison of the

(25) Green, R. J.; Hopkinson, I.; Jones, R. A. L. *Langmuir* **1999**, *15*, 5102–5110.

(26) Giacomelli, C. E.; Norde, W. *J. Colloid Interface Sci.* **2001**, *233*, 234–240.

(27) Elghanian, R.; Storhoff, J. J.; Mucic, R. C.; Letsinger, R. L.; Mirkin, C. A. *Science* **1997**, *277*, 1078–1081.

(28) Lazarides, A. A.; Schatz, G. C. *J. Phys. Chem. B* **2000**, *104*, 460–467.

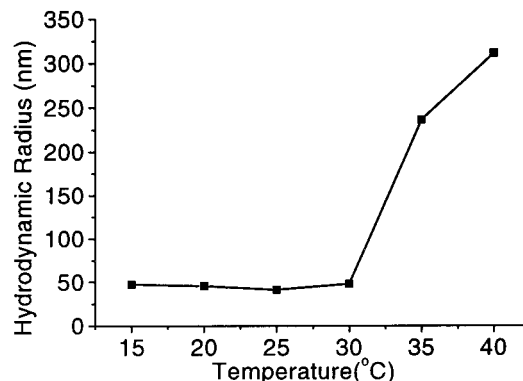


Figure 4. Change in the hydrodynamic radius (R_H) of Au-ELP as a function of temperature.

interfacial phase transition of adsorbed and covalently grafted ELPs as a function of interfacial chemistry and environmental stimuli will be presented elsewhere.

Because the increased absorbance in the 600–750 nm range is a clear optical signature of the formation of aggregates, the integrated absorbance between these wavelengths was used as a spectroscopic parameter of aggregate formation due to the interfacial phase transition of the ELP (Figure 2B). The temperature-dependent behavior of the ELP in solution (14 μ M) is also shown for comparison in the inset in Figure 2B. The thermal transition behavior of the ELP, adsorbed on gold colloids functionalized with a MUA SAM, and in solution is similar in terms of a sharp phase transition, although the phase transition on the surface is somewhat less reversible than that in solution and exhibits greater hysteresis. Because the transition temperature of ELPs in solution is an inverse logarithmic function of ELP concentration,¹⁷ it is difficult to directly compare the transition temperature on a surface with the solution transition temperature without an independent estimate of the effective local concentration of the ELP at the solid–water interface. The decrease in the transition temperature of adsorbed ELP relative to that in solution may be due to the higher effective concentration of ELP at the colloid–water interface. Moreover, energetically favorable interactions between the SAM and the ELP might also alter the transition temperature.

Because colloidal SPR is insensitive to small colloidal aggregates,^{29,28} a small continuous change in hydrophobicity with temperature may result in the formation of a low concentration of small aggregates that may be undetectable colorimetrically. We therefore investigated whether the sharp change in the absorbance observed by temperature-programmed UV–visible spectrophotometry of Au-ELP is in fact because of rapid hydrophobically driven aggregation of particles due to sharp phase transition of ELP, and is not an artifact arising from the analytical insensitivity of this method. Because it is very sensitive to the presence of small aggregates, we performed dynamic light scattering (DLS) as a function of temperature to independently examine colloidal aggregation, because it is very sensitive to the presence of small aggregates (Figure 4). The constant hydrodynamic radius (R_H) of \sim 45 nm as the temperature was increased from 15 to 30 °C excludes the presence of small aggregates formed as a result of subtle structural changes that may be undetectable by UV–visible spectrophotometry. Upon further increase of temperature to 35 °C, larger aggregates appeared with a R_H of 236 nm. The sharp change in the R_H between 30 and 35 °C validates the hypothesis of rapid

(29) McConnell, W. P.; Novak, J. P.; Brousseau, L. C., III; Fuierer, R. R.; Tenent, R. C.; Feldheim, D. L. *J. Phys. Chem. B* **2000**, *104*, 8925–8930.

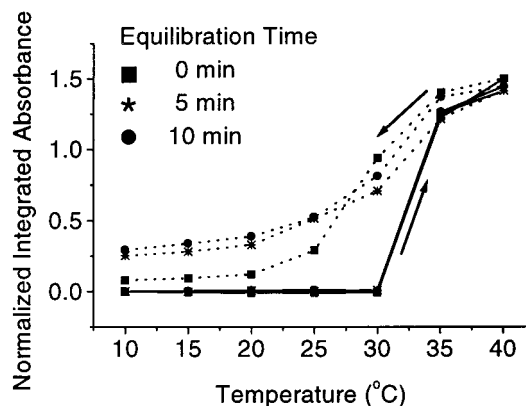


Figure 5. Influence of equilibration time on transition temperature and reversibility of Au-ELP. The absorbance spectra over 350–750 nm were collected after the samples were incubated at a specified temperature for the indicated time. Heating cycles are shown by solid lines while cooling cycles are shown by dotted lines.

aggregate formation due to the interfacial phase transition of adsorbed ELP. The presence of large aggregates is also consistent with previous observations that a strong absorbance at higher wavelengths is a consequence of a large, dense, and multilayered aggregation process.^{24,30} Due to the incomplete reversibility of the aggregation process, a mixed population of aggregates and dissociated colloids exists as the temperature is lowered that makes the DLS results difficult to interpret as the temperature was lowered from 40 to 10 °C (results not shown).

The effect of thermal equilibration time on hysteresis and reversibility of the interfacial phase transition was also investigated by colloidal SPR. Figure 5 shows that increasing the equilibration time from 0 to 10 min had no effect on the transition temperature, although the transition was less reversible for longer equilibration times. An identical transition temperature defined by the inflection point of the NIA versus T profiles, irrespective of the equilibration time, is consistent with a sharp phase transition profile of adsorbed ELP, similar to that in solution. Due to the longer time for which the colloidal sample is exposed to higher temperature at slower cooling rates, a larger fraction of the ELP may thermally denature, which may explain the lower reversibility of the transition for longer equilibration times.

An inverse dependence of the ELP transition temperature on NaCl concentration was also observed for Au-ELP, similar to that observed for ELPs in solution (results not shown).^{12,16} The decrease in the interfacial transition temperature of the ELP with increasing salt concentration is useful because it provides an experimentally convenient method to isothermally manipulate the surface phase transition.

The practical use of surface immobilized ELPs to fabricate environmentally reversible interfaces will depend, to a large extent, on the ability to reversibly cycle the immobilized ELP between its hydrophilic and hydrophobic state. We monitored the reversibility of the phase transition of Au-ELP, as the temperature was cycled between 20 ($T < T_i$) and 40 °C ($T > T_i$). Figure 6 shows that the ELP was successfully cycled between its hydrophobic and hydrophilic state up to six times, which clearly indicates that the surface phase transition of adsorbed ELP is highly reversible. However, the fraction of irreversibly aggregated ELP increased at 20 °C with every cycle. This was accompanied by a decreased concentration of aggregates at 40 °C in subsequent cycles. We believe that these

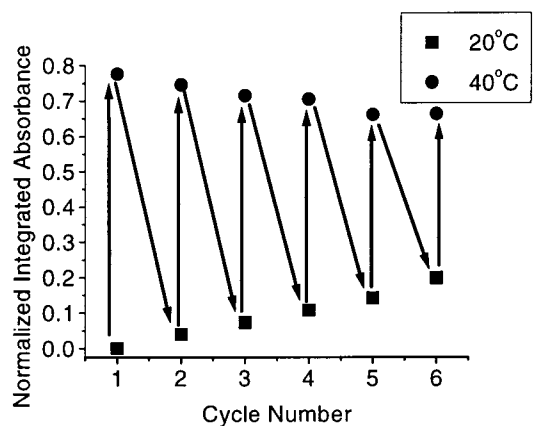


Figure 6. Reversibility of the interfacial phase transition of Au-ELP. The aggregation was monitored as the temperature of Au-ELP was cycled between 20 and 40 °C.

effects are due to the following competing processes. First, the partial reversibility of the aggregation process increases the number of aggregates with each cycle, and second, some irreversible adsorption of hydrophobic ELP–gold aggregates to the cuvette walls results in a decrease in the total number of colloidal particles, indicated by the formation of a violet film on the cuvette walls, when the aggregates were left in the cuvette for an extended period of time. We could not, however, separate the individual contributions of each of these processes to the absorbance spectrum.

Conclusions

Colloidal SPR of immobilized ELPs on functionalized Au nanoparticles provides an experimentally simple and convenient method to study the phase transition of immobilized ELPs at the solid–water interface. The primary advantage of this method is its extreme simplicity: gold nanoparticles are easily prepared, and their absorbance spectrum is easily measured in widely available, UV–vis spectrophotometers. Furthermore, because this colorimetric assay is carried out in aqueous medium, the influence of environmental factors such as the effect of cosolvents, cosolutes, and pH can be easily studied. The use of gold nanoparticles has several ancillary advantages as well; the spontaneous self-assembly of alkanethiols on gold allows convenient fabrication of surfaces with well-defined interfacial properties and reactive groups,³¹ which will enable the relationship between interfacial properties and the ELP phase transition to be systematically elucidated. We believe that this method should be generally applicable to other “smart” polymers that undergo hydrophilic–hydrophobic phase transitions in response to changes in their environment.

Although colloidal SPR enables easy determination of the transition temperature of immobilized, environmentally responsive polymers, it has two limitations: First, the phase transition must be accompanied by a change in hydrophobicity of the polymer leading to colloid aggregation. Second, colloidal SPR is a colorimetric method that does not provide information on the changes in molecular conformation of the polymer and water desolvation that often accompany interfacial transitions.³² It is therefore likely to be most useful in concert with complementary

(31) Ostuni, E.; Yan, L.; Whitesides, G. M. *Colloids Surf. B* **1999**, *15*, 3–30.

(32) *Proteins at interfaces II*; Horbett, T. A., Brash, J. L., Eds.; American Chemical Society Symp. Ser. 602; American Chemical Society: Washington, DC, 1995.

(30) Shipway, A. N.; Lahav, M.; Gabai, R.; Willner, I. *Langmuir* **2000**, *16*, 8789–8795.

spectroscopic techniques, such as infrared spectroscopy³³ and sum-frequency-generation,³⁴ that can probe the molecular details of interfacial transitions.

(33) *Biopolymers at Interface*; Malmsten, M., Ed.; Surfactant science series v 75; Marcel Dekker: New York, 1998.

Acknowledgment. This research was supported by the NIH, grant GM-61232, and a NSF CAREER award (BES-97-33009) to A.C.

JA015585R

(34) Bain, C. D. *Curr. Opin. Colloid Interface Sci.* **1998**, 3, 287–292.